RESEARCH ARTICLE

Saline Lacustrine Dolomitization and Reservoir Significance of the Tengger Formation in the Baiyinchagan Sag

Shengyu Li[1,2,*]

[1] School of Petroleum Engineering, Chongqing University of Science and Technology, Chongqing 401331, China
[2] Chongqing Key Laboratory of Complex Oil and Gas Field Exploration and Development, Chongqing University of Science and Technology, Chongqing 401331, China

Abstract

Continental saline lacustrine dolomite reservoirs remain less understood than their marine analogs. This study investigates the lower Cretaceous Tengger Formation in the western Baiyinchagan Sag, Erlian Basin, using core, thin section, SEM, XRD, isotope and petrophysical analyses. The dark muddy dolomitic rocks are composed mainly of ankerite, albite and natrolite with low clay content, indicating a mixed origin of saline lake evaporation and deep-sourced fluids. Two dolomitization types control reservoir quality: penecontemporaneous dolomitization creates intercrystalline pores, whereas burial dolomitization forms cements that block pores. Dissolution pores and high-angle fractures constitute the main storage space and permeability pathways. Laminated microcrystalline to finely crystalline dolomite exhibits the best properties, with average porosity of 13.8% and permeability of $1.56 \times 10^{-3}\,\mu\text{m}^2$. The semi-deep to deep lacustrine facies near syn-depositional faults are primary exploration targets. These findings provide a genetic model for saline lacustrine dolomite reservoirs and practical guidance for exploration in analogous basins.

Keywords: Baiyinchagan Sag, tengger formation, saline lacustrine basin, dolomite reservoir.

1 Introduction

The importance of dolomite reservoirs in deep and ancient marine strata has been widely recognized. In contrast, research on continental lacustrine dolomite has been relatively limited [1–3]. However, exploration practices over the past two decades indicate that Mesozoic-Cenozoic continental lacustrine dolomite in China also contains significant hydrocarbon potential, with commercial reserves discovered in several areas, including the Mahu Sag of the Junggar Basin and the Dongying Sag of the Bohai Bay Basin [4, 5]. A saline lacustrine basin is a special type of continental lake basin, typically characterized by water salinity greater than 3.5%, strong evaporation, water stratification, and elevated Mg/Ca ratios. According

Submitted: 17 May 2026
Accepted: 18 June 2026
Published: 25 June 2026

Vol. 2, **No.** 3, 2026.
10.62762/JGEE.2026.787396

***Corresponding author:**
✉ Shengyu Li
shyulili@qq.com; 2021005@cqust.edu.cn

Citation
Li, S. (2026). Saline Lacustrine Dolomitization and Reservoir Significance of the Tengger Formation in the Baiyinchagan Sag. *Journal of Geo-Energy and Environment*, 2(3), 219–229.

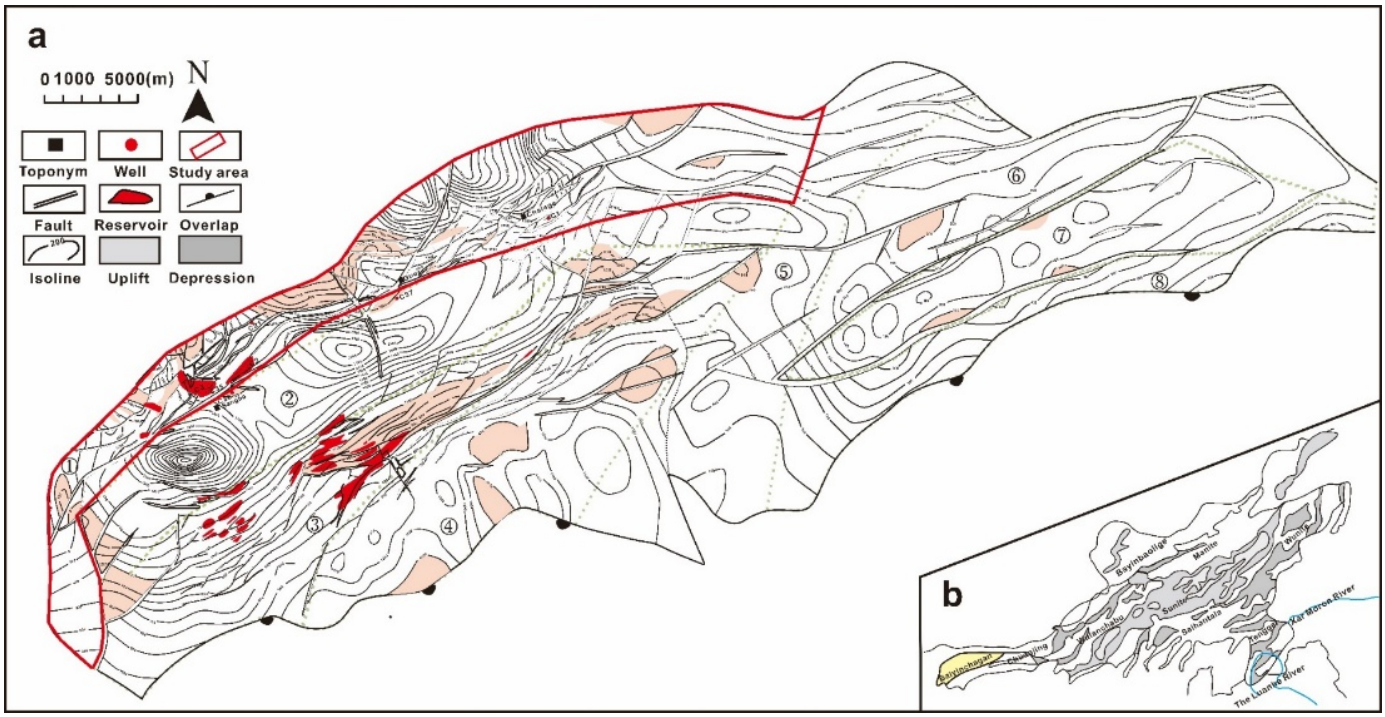

Figure 1. Geographical location and tectonic unit division of the study area. (a) Tectonic unit division and study area of the Baiyinchagan Sag; (b)Tectonic unit division of the Erlian Basin.

to water chemistry, saline lacustrine basins can be classified into carbonate type, sulfate type, and chloride type. In such environments, evaporative concentration increases lake water salinity, and when the Mg/Ca ratio exceeds a critical threshold, dolomite can form through chemical precipitation or penecontemporaneous metasomatism. Unlike marine dolomite, saline lacustrine dolomite is commonly associated with siliciclastic rocks, evaporites, and alkaline minerals, and exhibits stronger heterogeneity and a more complex diagenetic history. Therefore, classical research models developed for marine dolomite cannot be directly applied to continental saline lacustrine settings.

Several key issues remain to be addressed in the study of continental saline lacustrine dolomite. First, the genetic mechanisms of dolomite are debated. In saline lacustrine environments, dolomitization can occur during the penecontemporaneous period via evaporative pumping, during early diagenesis via penecontemporaneous metasomatism, or during burial via burial metasomatism [6, 7]. Different genetic types have distinct petrological and geochemical characteristics and contribute differently to reservoir quality [8–10]. For instance, in Early Cretaceous lacustrine basins with extensional tectonic backgrounds, microbial and hydrothermal processes interact to produce dolomites with contrasting crystal fabrics and pore systems [8]. In particular, the mineral assemblages and fabrics of hydrothermal-sedimentary rocks in the Erlian Basin record complex genetic processes involving both evaporative concentration and deep-sourced fluid input [1, 2]. The role of microbial activity and alkaline conditions in lacustrine dolomite formation has also been increasingly recognized. Sulfate-reducing bacteria operating under the anoxic, haloalkaline conditions of saline lakes generate local alkalinity and remove dissolved sulfate, thereby lowering the kinetic barrier to dolomite nucleation [11]. Abiotically-formed primary dolomite has additionally been documented in lacustrine settings where smectitic clay minerals catalyze dolomite ordering under evaporative alkaline conditions [12]. Second, the control of saline lacustrine evolution on dolomitization remains unclear. How variations in salinity, water chemistry, and sediment supply affect dolomite precipitation and preservation requires further investigation [14, 15]. Classical dolomite reservoir models emphasize the roles of evaporative pumping, seepage-reflux, and burial dolomitization in controlling pore evolution [15], but these concepts require substantial adaptation when applied to continental saline lacustrine settings, where siliciclastic inputs, alkaline authigenic minerals, and deep-sourced hydrothermal fluids introduce complexity absent from marine analogs. Isotopic studies of saline lacustrine dolomite

cements demonstrate that evaporative concentration of lake water generates Mg^{2+}-enriched diagenetic fluids that drive both penecontemporaneous and burial dolomitization, with the carbon and oxygen isotope compositions of the dolomite recording the salinity evolution of the basin [14]. The transition from acidic to alkaline diagenetic environments during burial, as documented in the Tengger Formation, significantly influences mineral stability and porosity evolution [25, 26]. Third, the relationship between dolomitization and reservoir quality needs to be clarified. Whether dolomitization is constructive or destructive for reservoir porosity depends on the timing, intensity, and subsequent diagenetic modification [16–18]. In the Baiyinchagan Sag, penecontemporaneous dolomitization creates intercrystalline pores that enhance reservoir quality, whereas burial dolomitization often forms cements that block pores [27]. Fractures and dissolution associated with hydrothermal activity also play a critical role in improving permeability [17, 19, 22, 24]. In both marine and lacustrine carbonate systems, syn-depositional faults serve as conduits for Mg-rich hydrothermal fluids and exert primary control on the spatial distribution, crystal fabric, and pore development of hydrothermal dolomite reservoirs [13]. In the Erlian Basin, syn-sedimentary hydrothermal fluids discharged along syn-depositional fault zones generated four petrographically distinct dolomite types, with coarse-crystalline fracture-infilling dolomite representing the highest-temperature fluid phase and creating the most permeable pathways [19]. Comparable patterns of dolomitization exerting dual constructive and destructive controls on porosity and permeability have been documented in carbonate reservoirs elsewhere: fabric-retentive early dolomitization preserves intercrystalline porosity against compaction, whereas late-stage burial cements occlude pore throats, a relationship that holds across depositional environments [20, 21]. In lacustrine mixed carbonate-siliciclastic successions across Chinese continental basins, the net effect of diagenesis on reservoir quality is governed by the relative timing and intensity of each diagenetic phase [23]. Furthermore, the strong heterogeneity of saline lacustrine dolomite reservoirs necessitates integrated petrophysical and geochemical approaches for accurate characterization and sweet spot prediction [23, 30]. Saline alkaline lacustrine settings with complex dolomite genesis—including evaporative, microbial, and hydrothermal pathways—require multi-proxy geochemical constraints to distinguish dolomitization mechanisms and their effects on reservoir quality [28, 29].

The Lower Cretaceous Tengger Formation in the Baiyinchagan Sag of the Erlian Basin hosts a typical continental saline lacustrine dolomite reservoir [25, 26]. Previous studies have confirmed that this dolomite has good hydrocarbon shows and exploration potential, but systematic understanding of how dolomitization controls reservoir development is still lacking. Based on previous work, this study takes the Tengger Formation in the western sub-sag of the Baiyinchagan Sag as the research object, and integrates core observation, thin-section petrography, scanning electron microscopy, X-ray diffraction, petrophysical analysis, and geochemical testing to systematically investigate the control of dolomitization on reservoir quality under saline lacustrine conditions and its implications for hydrocarbon exploration. The results are expected to deepen the understanding of dolomitization in continental saline lacustrine basins and provide a theoretical basis for exploration in the Baiyinchagan Sag and analogous basins.

2 Geological Setting

The Baiyinchagan Sag, located in the western part of the Erlian Basin in northern China, is a typical Mesozoic and Cenozoic continental rift basin [30] (Figure 1(a, b)). The sag extends in a NE to SW direction and exhibits a classic north faulted south onlapped half graben structure, bounded by major boundary faults in the north and onlapping the uplift in the south. The western sub sag is the main hydrocarbon generation center of the Baiyinchagan Sag.

During the deposition of the Tengger Formation, the study area was under an arid to semi arid paleoclimatic condition, with evaporation exceeding precipitation. This climatic condition, combined with the semi closed hydrological system of the lake basin, led to the formation of a saline lacustrine environment. The sedimentary systems of the Tengger Formation include fan deltas, braided river deltas, lacustrine facies, and turbidite fans. From the basin margin to the center, the sedimentary environments transition from fan deltas in the northern steep slope and braided river deltas in the southern gentle slope to shore shallow lacustrine, and finally to semi deep to deep lacustrine facies. Dolomites are mainly distributed in the semi deep to deep lacustrine facies, concentrated near the NE trending syndepositional fault zones in the center

Table 1. Calculation results of paleosalinity in the Baiyinchagan Sag.

Stratigraphic	Samples	K_2O (%)	B (ppm)	Adjusted B (ppm)	Equivalent B (ppm)	Paleosalinity (%)
K_1bd_1	1	2.29	51.93	192.75	160	8.59
K_1bd_2	3	2.30	95.29	352.16	270	19.34
K_1bd_3	4	3.06	97.76	271.56	220	14.45
K_1bt	5	2.31	91.48	336.61	260	18.36
K_1ba_2	3	2.16	78.83	310.21	240	16.41
K_1ba_1	1	1.61	77.28	408.00	275	19.82

Table 2. Statistical table of inorganic element content ratio in the Tengger Formation.

Well	Depth (m)	B/Ga	Sr/Ba	Sr/Ca	Fe/Mn	V/(V + Ni)	V/Cr
C1	1526.25	3.38	1.60	0.0224	43.47	0.78	2.7
C1	1866.43	2.43	0.62	0.0144	125	0.88	2.14
C2	1268.56	4.42	4.18	0.0158	32.26	0.67	1.69
C2	1496.86	2.59	0.35	0.0447	25	0.9	1.52
C2	2151.4	3.23	0.41	0.0089	125	0.85	2.56
C3	1326.90	2.56	0.56	0.0516	62.5	0.72	2.00
C35	1555.88	2.07	0.67	0.0392	90.9	0.75	1.78
C36	1556.95	2.41	0.71	0.0134	142.85	0.66	1.59

of the sub sag.

3 Methodology

Sampling avoided lithological transitions, weathered surfaces, and special structures. Representative core samples were prepared as 0.03 mm standard thin sections and blue epoxy casting thin sections. A polarizing microscope was used to identify dolomite crystal size, shape, euhedral degree, intercrystalline pores and dissolution features, to distinguish microcrystalline, very fine crystalline and fine crystalline textures, to recognize fracture types and fillings, and to estimate areal porosity. For scanning electron microscopy, samples were cut, ground, polished, ultrasonically cleaned and carbon coated. Dolomite micro-morphology, intercrystalline micropores, nano-scale pores and authigenic mineral occurrences were observed under backscattered and secondary electron modes. Whole-rock X-ray diffraction quantified the relative contents of dolomite, calcite, ankerite, albite, natrolite, barite, pyrite and clay minerals. Major and trace elements were analyzed by X-ray fluorescence and inductively coupled plasma mass spectrometry, calculating Mg/Ca, Sr/Ba, Fe/Mn and B/Ga ratios to constrain paleosalinity, paleotemperature and redox conditions. Fluid inclusions coexisting with dolomite and associated cements were analyzed. Primary inclusions were selected under a polarizing microscope, and microthermometric measurements were performed using a heating-freezing stage to obtain homogenization and ice melting temperatures, from which fluid salinities were calculated.

4 Results and Discussion

4.1 Dolomite Genesis and Multi-stage Diagenetic Environment Evolution

The upper member of the Lower Cretaceous Tengger Formation to the first member of the Duhongmu Formation in the Baiyinchagan Sag consists of a thick sequence of dark muddy dolomitic rocks, including argillaceous dolostone, dolomitic mudstone and dolomite, which are mainly distributed in the central deep sag. These lithologies show typical deep lacustrine sedimentary features and develop massive, laminated and granular structures. Different from ordinary muddy dolomitic rocks, this rock sequence has a low content of platy clay minerals. It is dominated by microcrystalline to cryptocrystalline ankerite and albite, as well as fine- to coarse-crystalline natrolite, with minor barite, ferripyrophyllite and pyrite. Albite within these muddy dolomitic rocks mostly occurs as micritic to microcrystalline grains dispersed in the rock matrix as a major constituent, and locally forms veinlets, with associated minerals including ankerite, K-feldspar, pyrite and clay minerals. Ankerite is predominantly microcrystalline, occurring in disseminated or laminated forms within the matrix; a small amount

exists as fine- to medium-crystalline grains, with natrolite being the primary associated mineral. Natrolite is mainly fine- to medium-crystalline and occurs either independently or in paragenesis with ankerite, barite, ferripyrophyllite and pyrite. Pyrite is widely developed, scattered throughout the matrix and distributed along grain boundaries. This mineral assemblage is characteristic of alkaline, high-salinity and reducing sedimentary environments, and is commonly found in lacustrine deposits affected by deep-sourced fluids. It indicates that the studied rocks have a dual genesis, formed by evaporative concentration within a saline lacustrine basin combined with the input of deep-sourced fluids. Paleosalinity calculated via the illite boron correction method indicates that the water body of the Baiyinchagan Sag remained persistently hypersaline during deposition of the Tengger to Duhongmu Formations. Salinity ranged from 8.59‰ to 19.82‰, with an average of approximately 16.16‰, corresponding to brackish to saline (mesohaline) conditions. The salinity also exhibited an overall upward-increasing trend, which provided favorable chemical conditions for evaporative dolomitization in the lake basin (Table 1).

In terms of rock fabric, the micritic texture consists of a mixture of micritic ankerite, microcrystalline albite and natrolite forming the matrix. The intraclastic texture is characterized by grains composed mainly of natrolite, ankerite and pyrite, with a matrix-supported cementation. Massive texture reflects rapid and continuous mineral precipitation, commonly occurring at the bottom of high-salinity stratified water bodies. Laminated texture is expressed as alternating micritic dolomite and feldspar laminae with dolomitic mudstone, indicating periodic changes in salinity or water chemistry. Scattered texture features 1 to 3 mm grains distributed in the dolomite matrix with stylolites. Filled vein and network textures show bedding planes and fractures filled by dolomite, zeolite and feldspar, reflecting fluid migration and precipitation along fractures during diagenesis. Syndepositional deformation textures exhibit local deformation at millimeter to centimeter scale, possibly related to seismic activity or soft-sediment deformation.

During deposition of the Tengger Formation, the lake basin gradually deepened, and ostracod assemblages reflect stable deep-water, moderately saline to brackish conditions. Palynological assemblages dominated by gymnosperm pollen indicate an arid subtropical to tropical paleoclimate. Element ratios B/Ga are mostly below 4.5, Sr/Ba mostly above 1, Fe/Mn all above 5 ranging from 20 to 400, Sr/Ca mostly above 0.01, and B values range from 77 to 200 ppm, indicating a continental depositional environment and high salinity. Paleosalinity calculated from boron content in illite after calibration gives a value of 18.36‰ for the Tengger Formation, belonging to polyhaline water. These arid, hot, brackish to saline conditions promoted evaporation and hydrolysis in the vadose zone, generating alkaline ions such as Ca^{2+}, Mg^{2+}, K^{+} and Na^{+}, so that the early diagenetic environment was overall slightly alkaline to alkaline (Table 2).

Elemental ratios (Table 2) further constrain the depositional environment. B/Ga ratios mostly below 4.5 indicate continental freshwater influence, while Sr/Ba values mostly above 1 and Sr/Ca above 0.01 confirm high salinity conditions. Fe/Mn ratios ranging from 25 to 142.85 suggest reducing bottom water conditions, consistent with the widespread occurrence of pyrite.

The Tengger Formation is a self-sourced and self-stored reservoir. The burial diagenetic stage experienced alternating acidic and alkaline conditions (Figure 2(a)). Dark mudstones have an average total organic carbon of 1.51% and vitrinite reflectance from 0.53% to 1.07% [26, 30], indicating the peak hydrocarbon generation stage. Basin modeling shows that at 113 Ma the paleotemperature reached 75°C and organic acids began to be generated; at 105 Ma the temperature reached 120°C with massive decomposition of short-chain carboxylic acids; the oil generation peak occurred at 100 Ma; and by 92 Ma the lower part of the Tengger Formation reached the overmature stage, decarboxylation weakened, and the diagenetic environment gradually shifted to alkaline conditions, which has persisted to the present. Three phases of hydrocarbon charging occurred at 113 Ma, 102 Ma and 97 Ma. Fluid inclusions show two distinct salinity endmembers (Figure 2(b)). Type I inclusions precipitated from low-temperature, high-salinity fluids, with homogenization temperatures ranging from 81.8 to 97.3°C and corresponding salinities of 8.01% to 9.60%. Type II inclusions were trapped within high-temperature, low-salinity fluid systems, featuring homogenization temperatures of 99.4 to 141.4°C and relatively low salinities between 3.99% and 6.30%. The transition from Type I to Type II inclusions record the geological evolution of strata from shallow burial to deep-burial diagenesis after sediment deposition. Hydrocarbon-bearing aqueous

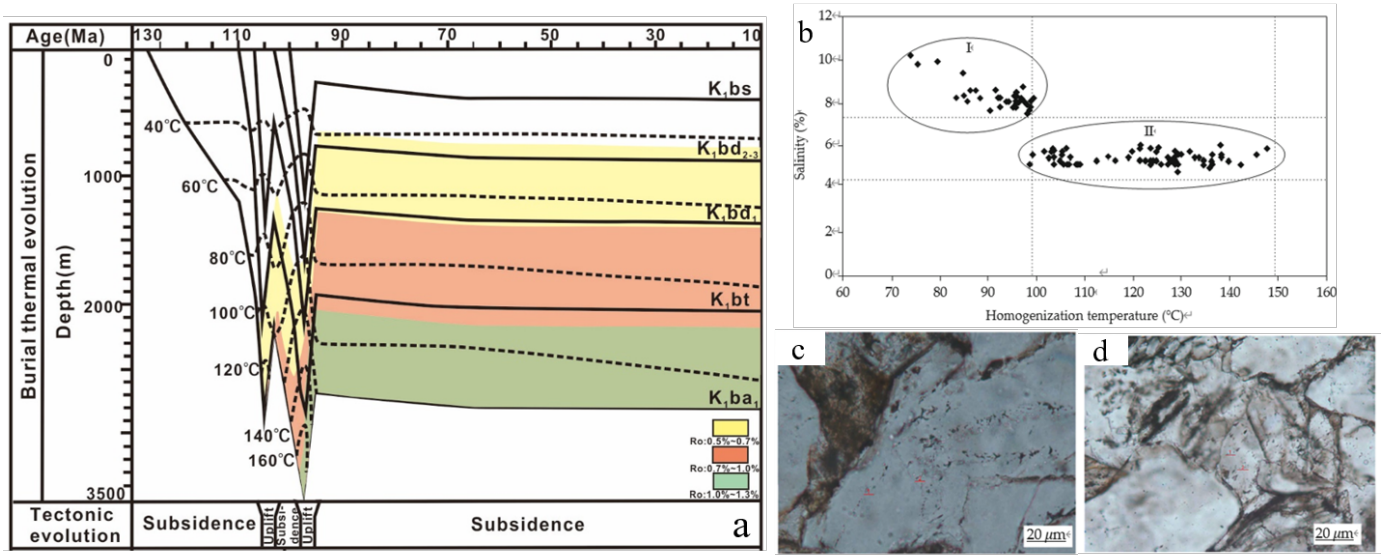

Figure 2. Burial thermal evolution and fluid inclusion characteristics of Tengger Formation reservoirs in the Baiyinchagan Sag. (a) Burial–thermal evolution history of the western sub-sag showing paleotemperature milestones at 113 Ma, 105 Ma, 100 Ma and 92 Ma and three hydrocarbon charging phases; (b) Homogenization temperature versus salinity biplot for fluid inclusions hosted in Tengger Formation reservoir cements, distinguishing Type I low-temperature high-salinity inclusions (T_h = 81.8–97.3°C, salinity = 8.01–9.60%) from Type II high-temperature low-salinity inclusions (T_h = 99.4–141.4°C, salinity = 3.99–6.30%); (c) Well C21, 1193.38 m: light-brown hydrocarbon-bearing aqueous inclusion clusters in Tengger Formation calcite cements; (d) Well C37, 1632.43 m: hydrocarbon-bearing aqueous inclusions in Tengger Formation calcite cements.

inclusions occur in Tengger Formation calcite cements of Well C21 (Figure 2(c)) and Well C37 (Figure 2(d)). The acidic diagenetic environment mainly resulted from acidic fluids expelled from source rocks, whereas the alkaline diagenetic environment originated from high-maturity organic matter and from deep-seated Paleozoic fault activities driving hydrothermal fluids upward along syn-depositional faults. These characteristics indicate a mixed origin of the muddy dolomitic rocks, combining evaporative concentration in a saline lacustrine basin with deep-sourced fluid activity.

4.2 Controls of Dolomitization on Reservoir Quality

Dolomitization in the Tengger Formation exerts dual controls on reservoir quality, being constructive or destructive depending on the type of dolomitization, diagenetic stage and intensity. Penecontemporaneous dolomitization occurred during the early stage of deposition, forming microcrystalline to finely crystalline dolomite under evaporative concentration in a saline lacustrine basin. This dolomite occurs as dispersed crystals or thin laminae in the matrix, with fine crystal size and well-developed intercrystalline pores, playing a constructive role in reservoir quality. Burial dolomitization occurred during the middle to late diagenetic stage, associated with deep-sourced fluid activity, forming medium- to coarse-crystalline dolomite that commonly occurs as cements filling fractures or pores. When excessively developed, this type reduces reservoir quality. Core and thin-section observations directly reveal various reservoir spaces and filling characteristics developed in dolomitic mudstones of the Tengger Formation from Well Xi26. At 1812 m, oil-bearing gypsum vugs are widely developed in dolomitic mudstones (Figure 3(a)). EDS spectra show major elements O, Si, Al, Ca, Mg, Na, K, plus minor Ti and Fe. High Si and Al denote terrigenous mud matrix; abundant Ca and Mg confirm dolomite growth, while Na records saline lacustrine sedimentary fluids (Figure 3(b)). At 1811.38 m, oil-saturated dissolution vugs (Figure 3(c)) and fractures filled with fibrous gypsum (Figure 3(d)) are identified, alongside abundant intragranular oil-saturated pores (Figure 3(e)). Oil-saturated microfractures occur at a depth of 1826.80 m (Figure 3(f)).

Constructive effects mainly include porosity creation through dissolution and porosity preservation by early dolomitization. Intercrystalline dissolution pores are the most common pore type, formed by mild dissolution along dolomite crystal boundaries. They are particularly well developed in microcrystalline

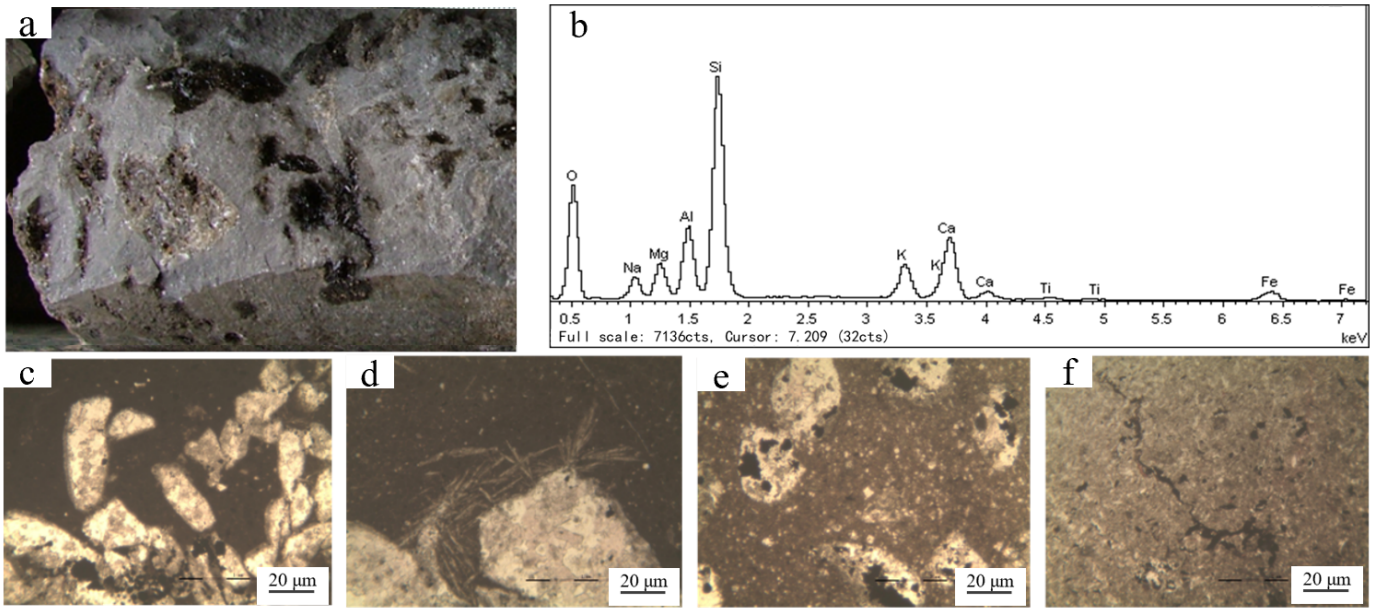

Figure 3. Core characteristics and EDS analysis of Tengger Formation reservoirs in Well Xi26. (a) Well Xi26, 1812m, Tengger Formation: dolomitic mudstone with oil-bearing gypsum vugs; (b) Well Xi26, 1818.83m: energy spectrum data acquired at the red cross position; (c) Well Xi26, 1811.38m, Tengger Formation: oil-saturated vugs; (d) Well Xi26, 1811.38m, Tengger Formation: fractures filled with fibrous gypsum; (e) Well Xi26, 1811.38m, Tengger Formation: developed intragranular oil-saturated vugs; (f) Well Xi26, 1826.80m, Tengger Formation: developed oil-saturated microfractures.

to finely crystalline dolomite, generally with pore diameters from 0.5 to 2 μm and plane porosity from 5% to 10%. Selective dissolution of soluble components such as feldspar, zeolite and calcite generates moldic pores and vugs. These dissolution features are especially developed near fault zones because fractures enhance acidic fluid circulation. Vugs range from 1 to 5 mm in diameter and, although less numerous, contribute significantly to storage space. Early dolomitization replaced metastable calcium carbonate before significant compaction, thereby preserving primary porosity. Intercrystalline micropores are generally smaller than 1 μm and are numerous, forming the matrix porosity part of the medium porosity ultra-low permeability system. According to petrophysical statistics from core samples across wells C1, C2, C3, C35 and C36 in the western sub-sag, samples with dolomite content exceeding 50% have an average porosity of 14.2%, whereas those with dolomite content below 30% have an average porosity of only 6.8%, indicating a positive correlation between the degree of dolomitization and porosity.

Destructive effects include excessive dolomite cementation during the late diagenetic stage and compaction. Burial dolomite cements often form overgrowths around early dolomite rhombs, blocking intercrystalline pores and throats. In some samples, sparry calcite infilling of vugs completely destroys the original storage space. Compaction, particularly in argillaceous dolomite intervals, reduces pore space by reorienting platy minerals and squeezing the soft matrix. Microscopically, bending and deformation of mica flakes and oriented alignment of the clayey matrix provide evidence of compaction. Statistics show that samples with mud content above 50% have an average porosity of only 4.2%, much lower than that of dolomite-rich rocks. Fractures, especially high-angle tectonic fractures, play a critical role in reservoir quality. Three fracture generations are recognized in the study area. Early diagenetic fractures parallel bedding and are mostly filled by calcite. Middle-stage tectonic fractures are mainly high-angle, with long extension and large aperture, serving as the main flow pathways. Late-stage pressure-solution fractures are stylolitic and contribute modestly to connectivity. Although fracture porosity is generally less than 1%, fractures connect isolated dissolution pores and intercrystalline micropores, forming an effective pore network and increasing permeability by one to two orders of magnitude. Imaging logs and thin sections from Well Xi31 clearly display fracture characteristics and syndepositional deformation structures (Figure 4(a)). Syndepositional plastic deformation structures occur at 2080.04 m (Figure 4(b)); abundant fractures

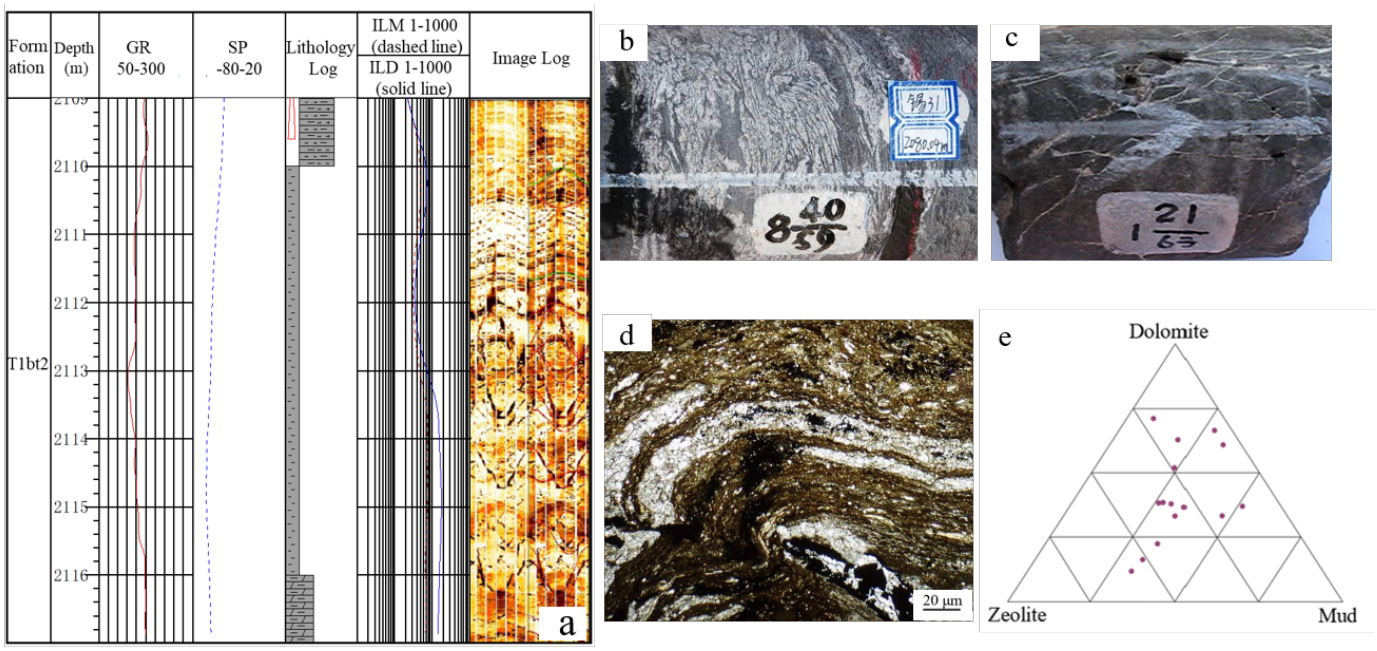

Figure 4. Characteristics of syndepositional deformation structures and fractures in the K_1bt Formation, Well Xi 31, Baiyinchagan Sag. (a) Conventional and image logs of the fracture-developed interval in Well Xi 31; (b) Well Xi 31, 2080.04m: Syndepositional plastic deformation structures; (c) Well Xi31, 2014.01m, K_1bt Formation: developed fractures in dolomitic mudstone; (d) Well Xi31, 2076.84m, Syndepositional deformation structures; (e) Lithology composition classification diagram of the upper K_1bt3 to upper K_1bt2 Members.

are developed in dolomitic mudstone at 2014.01 m (Figure 4(c)); syndepositional deformation features are observed at 2076.84 m (Figure 4(d)). The ternary diagram of dolomite-mud-zeolite illustrates that samples from upper K_1bt_2 to upper K_1bt_3 Members are mainly concentrated near the dolomite apex, dominated by dolomitic mudstone and muddy dolomite. Mud components are ubiquitous while zeolite generally occurs in low proportions, with only a few samples enriched in mud and zeolite, revealing mineral compositional variation of saline lacustrine mixed sediments (Figure 4(e)).

Petrophysical measurements on core plug samples from the study wells reveal that different lithofacies have markedly different reservoir properties. Laminated microcrystalline to finely crystalline dolomite has the best properties, with average porosity of 13.8% and average permeability of 1.56×10^{-3} μm^2 (equivalent to 1.56 mD), and its main storage spaces are intercrystalline dissolution pores and microfractures. Massive micritic dolomite is second, with average porosity of 10.2% and average permeability of 0.42×10^{-3} μm^2, dominated by intercrystalline pores. Argillaceous dolomite has poor properties, with average porosity of 6.5% and average permeability of 0.18×10^{-3} μm^2, due to strong compaction and weak dissolution. Dolomitic mudstone has the poorest properties, with average porosity of 3.8% and average permeability of 0.06×10^{-3} μm^2, relying mainly on fractures to improve flow capacity.

4.3 Reservoir Development Model and Exploration Implications

Based on the above analysis, a four-stage development model is proposed for the dolomite reservoir of the Tengger Formation in the western sub-sag. Stage one is the formation of the saline lacustrine basin under an arid to semiarid paleoclimate, where strong evaporation increased salinity and the Mg/Ca ratio, and syn-depositional faults controlled the depocenter geometry and provided pathways for deep-sourced fluids. Stage two is early dolomitization and porosity preservation. In the semi-deep to deep lacustrine environment, elevated Mg/Ca ratio and alkaline pH triggered penecontemporaneous dolomitization, while deep-sourced fluids supplied additional Mg^{2+} and Fe^{2+}, forming microcrystalline to finely crystalline dolomite with abundant intercrystalline micropores that resisted compaction. Stage three is dissolution and fracture development. Two phases of dissolution occurred: early meteoric water dissolution during short humid periods, and burial organic acid dissolution during source rock maturation. Tectonic

activity generated high-angle fractures, and pressure solution formed low-angle reticulate fractures. Fractures connected isolated pores and significantly improved permeability. Stage four is hydrocarbon charging and late diagenetic modification. Three phases of hydrocarbon charging occurred at 113 Ma, 102 Ma and 97 Ma. Early charging partly inhibited cementation, preserving porosity. The resulting reservoir exhibits medium porosity and ultra-low permeability, with strong heterogeneity and complex oil-water distribution.

This study has several implications for hydrocarbon exploration. The semi-deep to deep lacustrine facies in saline lacustrine basins should be the primary target for dolomite reservoir exploration. Areas near syn-depositional faults are most favorable because faults provide pathways for deep-sourced fluids, enhance permeability through fractures, and promote dissolution. Among dolomite lithofacies, laminated microcrystalline to finely crystalline dolomite with intercrystalline dissolution pores and microfractures is the best reservoir rock. Given that the western sub-sag is the only hydrocarbon-generating depocenter, any dolomite body with reasonable porosity and fracture connectivity in this area has high exploration potential. However, the strong heterogeneity requires integrated seismic, logging and geological analyses for sweet spot prediction.

5 Conclusion

The lower Cretaceous Tengger Formation in the western Baiyinchagan Sag hosts muddy dolomitic rocks of mixed saline lacustrine and deep-sourced fluid origin. Penecontemporaneous dolomitization is constructive for reservoir quality by generating intercrystalline pores, whereas burial dolomitization is often destructive by occluding pores. Dissolution pores and high-angle fractures constitute the effective pore-fracture network. Laminated microcrystalline to finely crystalline dolomite is the most favorable lithofacies for exploration. The semi-deep to deep lacustrine facies adjacent to syn-depositional faults are the primary targets, and the western sub-sag has high exploration potential due to its hydrocarbon generation capability.

Data Availability Statement

Data will be made available on request.

Funding

This work was supported in part by the Natural Science Foundation of Chongqing, China under Grant CSTB2022NSCQ-MSX1402; in part by the Science and Technology Research Program of the Chongqing Municipal Education Commission, China under Grant KJQN202301549; in part by the Open Fund of SINOPEC Key Laboratory of Acid Gas Field Development under Grant 31300027-25-ZC0613-0029; in part by the Open Fund of SINOPEC Key Laboratory of Marine Oil and Gas Reservoir Development under Grant 33550000-26-ZC0609-0006.

Conflicts of Interest

The authors declare no conflicts of interest.

AI Use Statement

The authors declare that no generative AI was used in the preparation of this manuscript.

Ethical Approval and Consent to Participate

Not applicable.

References

[1] Zhong, D. K., Yang, Z., Sun, H. T., & Zhang, S. (2018). Petrological characteristics of hydrothermal-sedimentary rocks: a case study of the Lower Cretaceous Tengger Formation in the Baiyinchagan sag of Erlian Basin, Inner Mongolia. *Journal of Paleogeography, 20*(1), 20-32. http://www.gdlxb.cn/CN/10.7605/gdlxb.2018.01.002

[2] Zhenmeng, S., Zheng, Q. I. A. N., & Xiancai, L. (2017). Reservoir property of the special lithologic section in the Lower Tengger Formation of A'nan Depression, Erlian Basin. *Geological Bulletin of China, 36*(4), 644-653. [CrossRef]

[3] FU, X., ZHANG, T., WU, J., WANG, X., ZHOU, J., JIANG, T., ... & LI, C. (2021). Characteristics and main controlling factors of tight oil reservoirs in Cretaceous Tengger Formation, A'nan Sag, Erlian Basin. Experimental Petroleum Geology, 43(1), 64-76. [CrossRef]

[4] Ma, B., Cao, Y., & Eriksson, K. A. (2020). Microbially induced dolomite precipitates in Eocene lacustrine siliciclastic sequences in the Dongying depression, Bohai Bay Basin, China: Evidence from petrology, geochemistry, and numerical modeling. *AAPG Bulletin, 104*(10), 2051-2075. [CrossRef]

[5] Wu, A., Cao, J., Zhang, J., Wu, T., & Wang, Y. (2022). Origin of microbial–hydrothermal bedded dolomites in the Permian Lucaogou Formation lacustrine shales,

Junggar Basin, NW China. *Sedimentary Geology, 440*, 106260. [CrossRef]

[6] Su, C., Zhong, D., Ma, Y., Huang, S., Qin, P., & Ren, X. (2022). Genesis of Lower Cretaceous lacustrine pistomesite in Baiyinchagan Sag, Erlian Basin, China: evidence from mineralogy and geochemical characteristics. *Arabian Journal of Geosciences, 15*(23), 1711. [CrossRef]

[7] Tao, M. E. N. G., Peng, L. I. U., Longwei, Q. I. U., Yongshi, W. A. N. G., Yali, L. I. U., Hongmei, L. I. N., & Changsheng, Q. U. (2017). Formation and distribution of the high quality reservoirs in a deep saline lacustrine basin: A case study from the upper part of the 4th member of Paleogene Shahejie Formation in Bonan sag, Jiyang depression, Bohai Bay Basin, East China. *Petroleum Exploration and Development, 44*(6), 948-959. [CrossRef]

[8] Zhang, K., Liu, Z., Xu, Z., Chang, Q., Fathy, D., Liu, R., & Bai, E. (2024). Microbial and hydrothermal dolomite formation in Early Cretaceous lacustrine sediments in Yin'e Basin: Insights from petrology and geochemistry. *Sedimentary Geology, 471*, 106739. [CrossRef]

[9] Wu, P., Dujie, H., Cao, L., Zheng, R., Wei, X., Ma, X., ... & Chen, J. (2023). Paleoenvironment and organic characterization of the lower Cretaceous lacustrine source rocks in the Erlian Basin: The influence of hydrothermal and volcanic activity on the source rock quality. *ACS omega, 8*(2), 1885-1911. [CrossRef]

[10] Guo, P., Wen, H., Li, C., He, H., & Sánchez-Román, M. (2023). Lacustrine dolomite in deep time: What really matters in early dolomite formation and accumulation?. *Earth-Science Reviews, 246*, 104575. [CrossRef]

[11] Sorokin, D. Y., Kuenen, J. G., & Muyzer, G. (2011). The microbial sulfur cycle at extremely haloalkaline conditions of soda lakes. *Frontiers in microbiology, 2*, 44. [CrossRef]

[12] Wanas, H. A., & Sallam, E. (2016). Abiotically-formed, primary dolomite in the mid-Eocene lacustrine succession at Gebel El-Goza El-Hamra, NE Egypt: An approach to the role of smectitic clays. *Sedimentary Geology, 343*, 132-140. [CrossRef]

[13] Guo, R., Zhang, S., Bai, X., Wang, K., Sun, X., & Liu, X. (2020). Hydrothermal dolomite reservoirs in a fault system and the factors controlling reservoir formation-A case study of Lower Paleozoic carbonate reservoirs in the Gucheng area, Tarim Basin. *Marine and Petroleum Geology, 120*, 104506. [CrossRef]

[14] Meng, H., Lv, Z., Shen, Z., & Xiong, C. (2018). Carbon and oxygen isotopic composition of saline lacustrine dolomite cements and its palaeoenvironmental significance: A case study of Paleogene Shahejie Formation, Bohai Sea. *Minerals, 9*(1), 13. [CrossRef]

[15] Davies, G. R. (1979). Dolomite reservoir rocks: Processes, controls, porosity development. In *Geology of Carbonate Porosity, Continuing Education Course Note Series 11* (pp. C1-C17). [CrossRef]

[16] Gawthorpe, R. L. (1987). Burial dolomitization and porosity development in a mixed carbonate-clastic sequence: an example from the Bowland Basin, northern England. *Sedimentology, 34*(4), 533-558. [CrossRef]

[17] Lei, Z., Hu, W., Xu, H., Xu, B., Cao, C., Cheng, C., & Zhu, Q. (2018). Characteristics of hydrothermal-structure-controlled fracture–vug dolomite reservoir and its influence on oil–water distribution: Lower Cretaceous, Baiyinchagan sag, Erlian Basin, North China. *Russian Geology and Geophysics, 59*(4), 405-418. [CrossRef]

[18] Gu, Y., Zhou, L., Jiang, Y., Jiang, C., Luo, M., & Zhu, X. (2019). A model of hydrothermal dolomite reservoir facies in Precambrian dolomite, Central Sichuan Basin, SW China and its geochemical characteristics. *Acta Geologica Sinica-English Edition, 93*(1), 130-145. [CrossRef]

[19] Yang, Z., Zhong, D., Whitaker, F., Lu, Z., Zhang, S., Tang, Z., ... & Li, Z. (2020). Syn-sedimentary hydrothermal dolomites in a lacustrine rift basin: Petrographic and geochemical evidence from the lower Cretaceous Erlian Basin, Northern China. *Sedimentology, 67*(1), 305-329. [CrossRef]

[20] Omidpour, A., Mahboubi, A., Moussavi-Harami, R., & Rahimpour-Bonab, H. (2022). Effects of dolomitization on porosity–Permeability distribution in depositional sequences and its effects on reservoir quality, a case from Asmari Formation, SW Iran. *Journal of Petroleum Science and Engineering, 208*, 109348. [CrossRef]

[21] El-Yamani, M. S., Al-Ramadan, K., & Cantrell, D. (2022). Diagenetic controls on porosity evolution and reservoir quality of an outcrop analogue of the Jurassic carbonate reservoirs in the Arabian Plate: An example from the Middle Jurassic Tuwaiq Mountain Formation, Central Saudi Arabia. *Journal of Petroleum Science and Engineering, 208*, 109669. [CrossRef]

[22] Yang, Z., Whitaker, F. F., Liu, R., Phillips, J. C., & Zhong, D. (2021). A new model for formation of lacustrine primary dolomite by subaqueous hydrothermal venting. *Geophysical Research Letters, 48*(6), e2020GL091335. [CrossRef]

[23] Wei, W., Azmy, K., & Zhu, X. (2022). Impact of diagenesis on reservoir quality of the lacustrine mixed carbonate-siliciclastic-volcaniclastic rocks in China. *Journal of Asian Earth Sciences, 233*, 105265. [CrossRef]

[24] Deng, Y. X., Ji, Y. L., Xu, S. M., Huang, P., & Guo, X. (2013). Characteristics and main controlling factors of Tenggeer Formation reservoir in Sanghe area, Baiyinchagan sag. *Acta Sedimentologica Sinica, 31*(2), 350-357. http://www.cjxb.ac.cn/article/id/933

[25] Li, S., Tian, J., Lin, X., Yin, N., Luo, C., & Yang, D. (2022). Reconstruction of the Diagenetic Environments of Tight Sandstone Reservoirs: A

Case Study from the Tengger Formation in the Baiyinchagan Sag, Erlian Basin, Northern China. *Lithosphere, 2022*(Special 9), 9220510. [CrossRef]

[26] Li, S., Tian, J., Lin, X., Zuo, Y., Kang, H., & Yang, D. (2020). Effect of alkaline diagenesis on sandstone reservoir quality: Insights from the Lower Cretaceous Erlian Basin, China. *Energy Exploration & Exploitation, 38*(2), 434-453. [CrossRef]

[27] Yang, Z., Zhong, D., Whitaker, F., Sun, H., Su, C., & Cao, X. (2021). Reservoir quality of tight oil plays in lacustrine rift basins: Insights from early Cretaceous fine-grained hydrothermal dolomites of the Erlian Basin, NE China. *Marine and Petroleum Geology, 124*, 104827. [CrossRef]

[28] Guo, P., Wen, H., & Sánchez-Román, M. (2023). Constraints on dolomite formation in a Late Palaeozoic saline alkaline lake deposit, Junggar Basin, north-west China. *Sedimentology, 70*(7), 2302-2330. [CrossRef]

[29] Zhang, S., Liu, Y. Q., Li, H., Jiao, X., & Zhou, D. W. (2020). Hydrothermal-sedimentary dolomite—a case from the Middle Permian in eastern Junggar Basin, China. *Journal of Palaeogeography, 9*(1), 24. [CrossRef]

[30] Tian, H., Ren, Z., Qi, K., Liu, J., Guo, S., Han, Z., ... & Zhu, L. (2025). Reservoir characteristics and diagenetic evolution of lower cretaceous in Baibei Sag, Erlian Basin, Northern China. *Processes, 13*(5), 1391. [CrossRef]

Shengyu Li received a PhD in Geology. She has led and participated in national major science and technology projects, projects funded by the Chongqing Natural Science Foundation, initiatives supported by the Chongqing Municipal Education Commission, and various industry–academia collaborative research programs. Her main research interests include unconventional petroleum geology and hydrothermal carbonate sedimentology. (Email: shyulili@qq.com; 2021005@cqust.edu.cn)